Spectroscopic Studies of Protein–Heme Interactions Accompanying the Allosteric Transition in Methemoglobins†

Eric R. Henry,*,‡,§,∥ Denis L. Rousseau,*,§ John J. Hopfield,§,∥,⊥ Robert W. Noble,# and Sanford R. Simon°

Laboratory of Chemical Physics, National Institutes of Health, Bethesda, Maryland 20205, AT&T Bell Laboratories, Murray Hill, New Jersey 07974, Department of Physics, Princeton University, Princeton, New Jersey 08544, Departments of Medicine and Biochemistry, State University of New York at Buffalo and Veterans Administration Hospital, Buffalo, New York 14215, and Department of Biochemistry, State University of New York at Stony Brook, Stony Brook, New York 11794

Received August 20, 1984; Revised Manuscript Received March 5, 1985

ABSTRACT: Resonance Raman, optical absorption, and circular dichroism spectroscopic techniques have been used to examine the effect of the addition of inositol hexaphosphate (IHP) to a series of carp and human methemoglobin derivatives. Markers of spin equilibrium in the high-frequency region (1450–1650 cm^{-1}) of the resonance Raman spectrum yield high/low-spin ratios consistent with direct magnetic susceptibility measurements. Changes in the low-frequency region (100–600 cm^{-1}) of the resonance Raman spectrum appear to correlate with the quaternary structure transition. Changes in the ultraviolet absorption spectra and the circular dichroism spectra also appear to be related to the quaternary structure change. By using the resonance Raman spin markers, we find that those derivatives of carp methemoglobin which are in spin equilibrium have a larger ratio of high-spin to low-spin populations than the corresponding derivatives of human methemoglobin. Upon the addition of IHP to the methemoglobins the spin equilibrium is shifted toward a larger high-spin population. This change in equilibrium is larger for the carp protein than for the human protein. We obtain an IHP-induced change in the free energy difference between the high-spin and low-spin states of 300 cal/mol for those human methemoglobins in which a quaternary structure change occurs and 600 cal/mol for carp methemoglobins. Our data are consistent with a quaternary structure change induced by IHP in all the carp methemoglobins studied (F^-, H_2O, SCN^-, NO_2^-, N_3^-, and CN^-) and in the F^-, H_2O, and SCN^- derivatives of the human protein but not in the NO_2^-, N_3^-, and CN^- derivatives. The Fe–CN stretching mode has been identified by isotopic substitution and found to be unchanged in frequency in carp CN^- metHb when the quaternary structure is changed. On the basis of our results we conclude that the protein forces at the heme due to the addition of IHP do not significantly affect the position of the iron atom with respect to the heme plane. Rather, the changes in spin equilibrium may be caused by protein-induced changes in the orientation of the proximal histidine or tertiary structure changes in the heme pocket which affect the porphyrin macrocycle. Either of these changes, or a combination thereof, leads to changes in the iron d orbital energies and concomitant changes in the spin equilibrium.

The physiological mechanisms of hemoglobin function are now well understood. In addition, descriptive models have been proposed to account for the observed thermodynamic and kinetic properties of hemoglobin ligand binding (Baldwin, 1975). However, the molecular basis for hemoglobin cooperativity remains to be solved. Stereochemical differences between deoxygenated and liganded hemoglobins have been detected from which molecular mechanisms have been inferred (Baldwin & Chothia, 1979), but the energies associated with these differences have not been determined. Also, the pathway by which the status of ligand binding at one heme is communicated to the protein and subsequently to other hemes remains to be determined. Various models for hemoglobin function have been proposed that place the free energy of cooperativity at the ligand binding site (Perutz, 1970; Baldwin & Chothia, 1979), at the subunit interfaces (Pettigrew et al., 1982), and distributed throughout the protein (Hopfield, 1973). The initial "trigger" in the pathway from the heme binding site to the subunit interface following ligand binding has been postulated to be the motion of the iron out of the heme plane (Baldwin & Chothia, 1979), movement of specific amino acid residues (Gelin & Karplus, 1977), and motion of a large core of atoms in the binding site region (Gelin et al., 1983). Spectroscopic studies appear to be the most promising means by which specific molecular interactions which bear on the energetics of cooperativity may be detected. In particular, such studies probe the conformational and electronic responses of the heme to globin structural changes (Rousseau & Ondrias, 1983) and, therefore, at least indirectly, the mechanism by which the protein controls the affinity for ligand binding at the heme.

The understanding of the structural basis for the cooperative transition in hemoglobin has been advanced by the study of the nonphysiological ferric form of hemoglobin, methemoglobin. Methemoglobins are useful to study because numerous ligands form stable methemoglobin complexes that have a wide range of electronic properties. In addition, organic phosphates such as inositol hexaphosphate (IHP)[1] bind to the

† Work done at Princeton University (E.R.H. and J.J.H.) was supported by NSF Grant DMR-80-15678. R.W.N. was the recipient of NIH Grant HL-12524 and research funds from the Veterans Administration. S.R.S. was the recipient of NIH Grant HL-25780.

* Address correspondence to E.R.H. at the National Institutes of Health or to D.L.R. at AT&T Bell Laboratories.

‡ National Institutes of Health.

§ AT&T Bell Laboratories.

∥ Princeton University.

⊥ Present address: Department of Chemistry, California Institute of Technology, Pasadena, CA 91125.

State University of New York at Buffalo and Veterans Administration Hospital.

° State University of New York at Stony Brook.

0006-2960/85/0424-5907$01.50/0

liganded methemoglobins and induce a change in quaternary structure in some but not in all methemoglobins. Several spectroscopic studies of methemoglobins have been reported (Perutz et al., 1974a,b, 1978; Asher et al., 1977; Scholler & Hoffman, 1979; Rousseau et al., 1980a; Nagai et al., 1980a; Cho et al., 1981), but general conclusions based on these reports are difficult to formulate because a complete systematic study of an extensive series of liganded methemoglobins is lacking. Therefore, we undertook an investigation of light absorption in the visible and ultraviolet regions, circular dichroism in the ultraviolet, and resonance Raman scattering properties of a large number of stable liganded derivatives of adult human and carp methemoglobins.

Experimental Procedures

Sample Preparation. Hb A and carp Hb were prepared by standard techniques (Allen et al., 1958; Tan et al., 1972). The hemoglobins were stored in solution at 4 °C in the oxy or carboxy form for use within 4 weeks or in the aquomet form for use within 2 weeks. The aquomet form was prepared by oxidizing oxyhemoglobin with nitrite ($NaNO_2$ in aqueous solution) or by photolyzing carboxyhemoglobin under strong light and an oxygen stream in the presence of nitrite. The nitrite was removed by passing the Hb solution down a Sephadex G-10 column.

Individual liganded methemoglobins were prepared by diluting a solution of aquomethemoglobin prepared as above in a pH-adjusted 0.1 M Bis-Tris buffer solution which was also 0.1 M in sodium or potassium salt of the required ligand. Isotopically substituted KSCN, KCN, and $NaNO_2$ salts were purchased from KOR Isotopes and used without further purification. The human methemoglobins were generally studied at pH 6.2–6.3, and the carp methemoglobins were studied at various points in the pH range 5.9–8. IHP, when required, was added as a concentrated buffered solution to the hemoglobin solutions, in 4–10-fold molar excess.

Samples for use with 413.1-nm excitation in the resonance Raman studies were prepared at concentrations of 50–100 μM in heme. Typical concentrations used in the optical studies were 200 μM for the methemoglobin A derivatives and 20–50 μM for the carp methemoglobin derivatives.

Instrumentation. The technique for the direct measurement of Raman difference spectra has been described in detail elsewhere (Rousseau, 1981; Shelnutt et al., 1981). Laser illumination of the samples for the Raman spectra used the 413.1-nm line from a Spectra-Physics 171 Kr^+ ion laser. All Raman spectra were measured at 2–4-cm^{-1} spectral slit widths.

All visible and UV absorption studies were performed at room temperature (22 °C) using a Cary 118 double-beam spectrophotometer. Samples were placed in spectrally matched Suprasil quartz cells of path length 1, 5, or 10 mm, manufactured by Hellma Cells. Base lines for the absorption difference spectra were adjusted to optimal flatness with the stripped form of the methemoglobin of interest in both the sample and reference compartments of the spectrophotometer.

CD spectra were measured on a Cary Model 60 spectropolarimeter with a Model 6001 CD attachment.

Results

Resonance Raman Spectra

Region at 1350–1400 cm^{-1}. The polarized line in the 1350–1400-cm^{-1} region of the Raman spectra of hemoglobins is strongly resonantly enhanced with laser excitation at 413.1 nm. This totally symmetric vibration is a porphyrin ring mode, with principal contributions from N–C_α bond stretches (Abe et al., 1978). The frequency of this vibration correlates with the oxidation state of the heme iron (Spiro & Strekas, 1974) and, in ferrous porphyrins, with π-electron back-donation into the porphyrin ring through the axial linkages (Spiro & Burke, 1976). It has also been shown to be sensitive to protein structure (Shelnutt et al., 1979).

The resonance Raman spectra in the 1350–1400-cm^{-1} frequency region were measured with 413.1-nm excitation (see paragraph at end of paper regarding supplementary material). Certain systematic features of the response of this mode to IHP binding to various methemoglobin A derivatives have already been noted (Rousseau et al., 1980a). For every methemoglobin A studied here this vibration displays a shift downward in frequency upon IHP binding to the protein. Those liganded methemoglobins A in which the iron is predominantly high spin (F^- and H_2O) exhibit a relatively large decrease (>0.6 cm^{-1}) in the frequency of this vibration when IHP is added. Those methemoglobins in which the iron is predominantly low spin (CN^- and N_3^-) display a smaller downward shift (about 0.2 cm^{-1}). For those liganded species in which a thermal mixture of high-spin and low-spin irons is present (NO_2^- and SCN^-), fairly large frequency shifts are seen, as well as significant changes in the shape of the line in each case.

Raman difference spectra of the carp methemoglobin derivatives in this region reveal striking changes in the shape and frequency of this line in several cases. N_3^-, NO_2^-, and SCN^- carp metHbs all show changes much larger than those seen in the corresponding methemoglobins A. In addition, SCN^-, H_2O, and F^- carp metHbs display a sensitivity of this line to changes in pH, without the addition of IHP.

Region at 1450–1650 cm^{-1}. Vibrations in the high-frequency region of the resonance Raman spectrum of methemoglobins are porphyrin ring modes (Spiro & Strekas, 1974). Raman lines at about 1480 and 1560 cm^{-1} are among those cited as indicators of a high-spin heme iron, whereas lines at about 1510 and 1580 cm^{-1} are used as low-spin indicators (Spiro & Strekas, 1974).

The high-frequency Raman spectra of the adult human and carp methemoglobins with 413.1-nm excitation are shown in Figures 1 and 2. The predominant features in these spectra are IHP-induced changes in relative intensities of lines, rather than changes in frequencies. The ±IHP difference spectra for CN^- and N_3^- metHb A indicate only very small changes in the high-frequency region for these ligands. On the other hand, the spectra of NO_2^-, SCN^-, and H_2O metHb A show significant changes in relative intensities of pairs of lines in the 1550–1600-cm^{-1} region and in the 1470–1530-cm^{-1} region. The spectrum of F^- metHb A shows an upward shift in the frequency of the line at 1564 cm^{-1} and a decrease in intensity of the line at 1479 cm^{-1}.

As in the 1350–1400-cm^{-1} region, the high-frequency Raman spectra of N_3^-, NO_2^-, and SCN^- carp metHb display large changes upon the addition of IHP. The spectrum of CN^- carp metHb shows IHP-induced intensity changes smaller than those shown by the other ligands but still somewhat larger than the changes seen in the spectrum of CN^- metHb A. The spectra of both H_2O and F^- carp metHb show relatively small IHP-induced changes in this region (at fixed pH) but a greater sensitivity to simple pH changes without IHP addition.

Low-Frequency Region. The nature of most vibrations in the region of the resonance Raman spectrum of hemoglobins

[1] Abbreviations: IHP, inositol hexaphosphate; Hb, hemoglobin; Hb A, adult human hemoglobin; metHb, methemoglobin; UV, ultraviolet; CD, circular dichroism; NMR, nuclear magnetic resonance; Bis-Tris, [bis(2-hydroxyethyl)amino]tris(hydroxymethyl)methane.

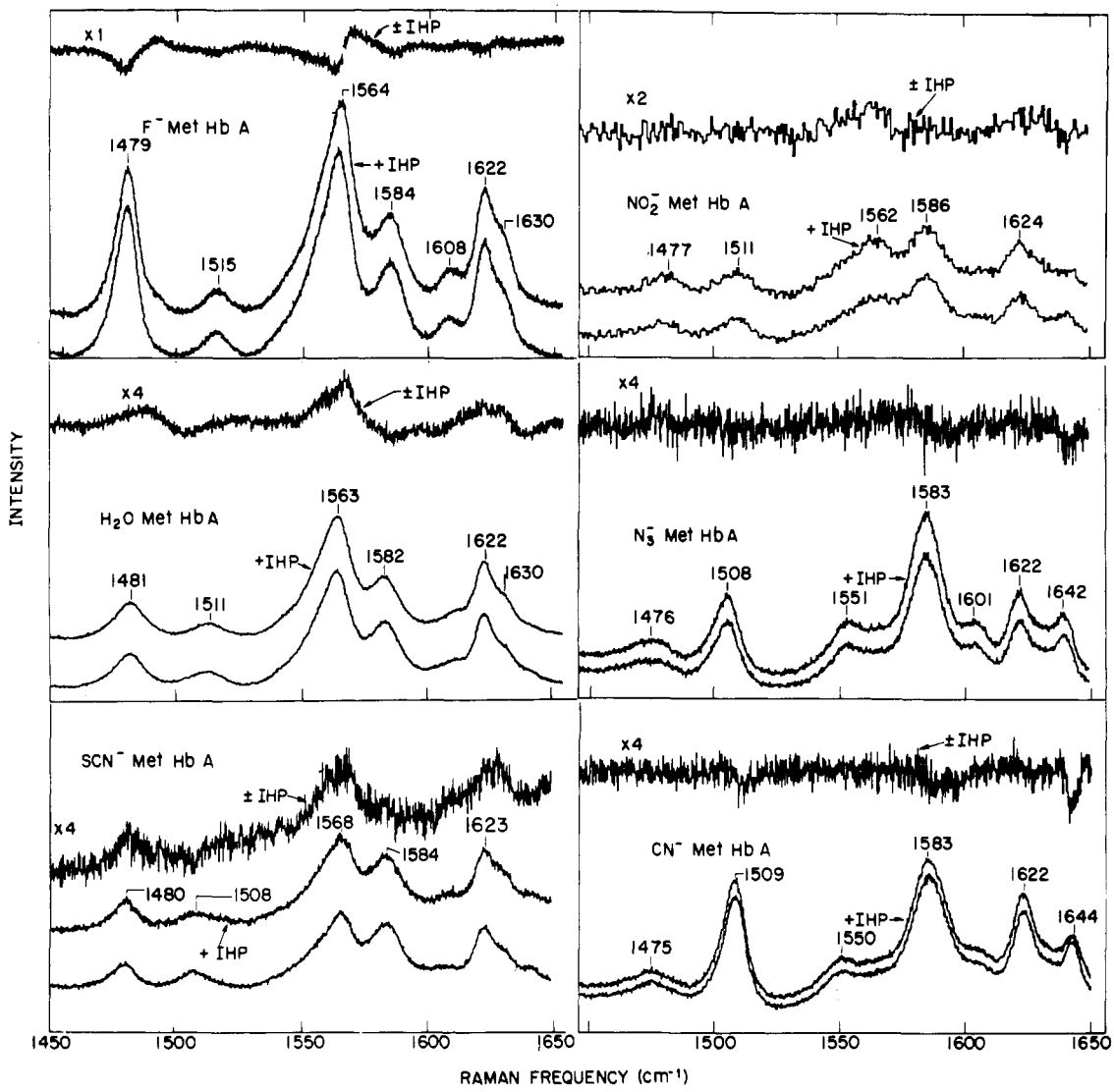

FIGURE 1: Resonance Raman spectra of liganded methemoglobin A derivatives in the high-frequency region. In each box, the difference spectrum of (+IHP) − (stripped) calculated from the pair of simultaneously obtained spectra is shown above the two spectra, scaled by the indicated factor. Conditions were 413.1-nm excitation at 50–200 mW, spectral slit width of 1–2 cm^{-1} (5–10 scans at 12–14 cm^{-1}/min), and heme concentration of 50–100 μM in 0.1 M Bis-Tris-buffered solutions, pH 6.3. The measurement for the NO_2^- derivative was made in a single scan at 96 cm^{-1}/min.

below about 600 cm^{-1} is not well-known, although this region is likely to include those porphyrin modes to which motions of the iron atom contribute significantly. It has recently been shown that out-of-plane modes in this region are resonantly enhanced (Choi & Spiro, 1983). The peripheral substituents also contribute to the normal coordinates in the low-frequency region (Choi et al., 1982a,b; Rousseau et al., 1983). The Raman spectra of various liganded adult human and carp methemoglobins in this region were measured (see paragraph at end of paper regarding supplementary material), and the spectra for the two F^- and the two CN^- derivatives are shown in Figures 3 and 4. The observed IHP-induced changes in the spectra of CN^-, N_3^-, and NO_2^- metHb A are quite small, whereas in the spectra of SCN^-, H_2O, and F^- metHb A the changes are distinctly larger and quite similar from ligand to ligand. These changes involve a downward shift in frequency by about 2 cm^{-1} of the line just below 350 cm^{-1} and changes in the frequencies of the pair of lines in the 350-400-cm^{-1} region such that the lower frequency line decreases in frequency and the higher frequency line increases in frequency. This is most clearly seen in the spectrum of F^- metHb A. In certain cases (most notably NO_2^- carp metHb) changes in the relative intensities of scattering in the 350- and 380-cm^{-1} regions are also seen. In the spectra of SCN^-, H_2O, and F^- metHb A, the line in the 680-cm^{-1} region experiences a distinct decrease in frequency.

The low-frequency resonance Raman spectra of the carp methemoglobins differ in some cases from those of the corresponding derivatives of methemoglobin A (notably in F^- and H_2O), but the IHP- (and pH change) induced changes in the spectra are qualitatively similar to those seen in the methemoglobins A. In the carp protein, however, the spectra of all of the liganded methemoglobins display these changes, including those liganded forms that in metHb A show little or no IHP-induced change in this region of the spectrum.

Isotopic Substitution Experiments. Several features in the resonance Raman spectra of hemoglobins have been clearly identified as modes involving the axial ligands of the heme iron. The Fe–O_2 stretch in oxyhemoglobin has been identified (Brunner, 1974), and the iron-proximal histidine stretch has been assigned in deoxyhemoglobin (Nagai et al., 1980b). In methemoglobins, the Fe–F stretch in F^- metHb, the Fe–OH stretch in OH^- metHb, and the Fe–N_3 stretch in N_3^- metHb have been assigned (Asher et al., 1977; Desbois et al., 1979). Isotopic substitutions of several ligands have been performed here in an attempt to identify additional ligand modes in methemoglobins using Raman difference spectroscopy. Figure 5a shows the simultaneously measured spectra of CN^- metHb

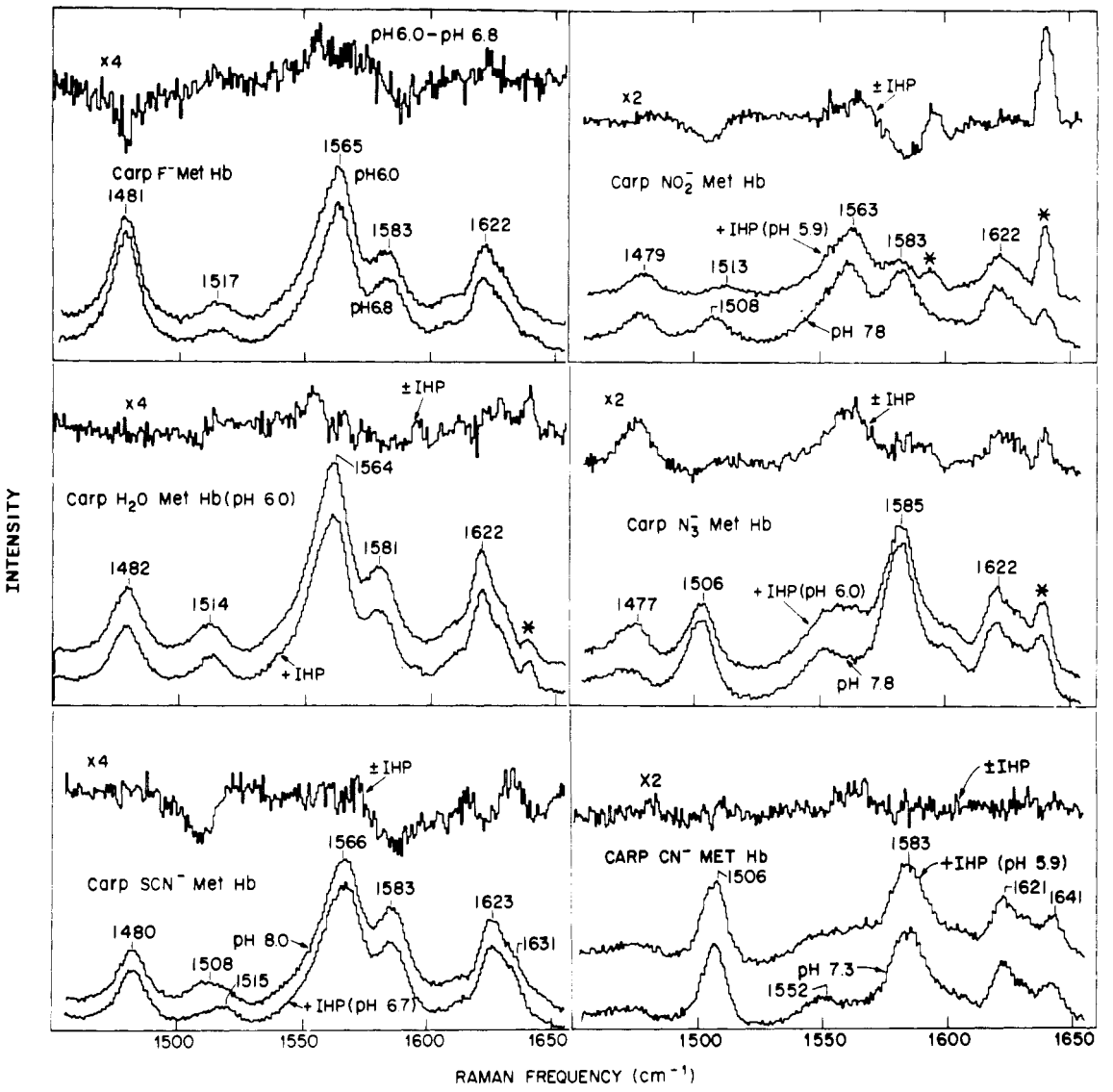

FIGURE 2: Resonance Raman spectra of carp methemoglobin derivatives in the high-frequency region. Conditions were the same as in Figure 1, except that the solution pH was 6.0 unless otherwise indicated. In addition, because of some photosensitivity exhibited by these derivatives, the number of scans and scan speed were adjusted so that total exposure time of the carp methemoglobin samples to laser illumination was kept to a minimum (usually less than 30 min). Each spectrum is labeled with the solution conditions (pH and the presence of IHP). Lines marked with an asterisk are laser fluorescence lines.

A with ^{14}N and ^{15}N in the ligand. The difference spectrum shows quite dramatically the lowering of the frequency of a single vibration at 452 cm^{-1} on substituting ^{15}N for ^{14}N in the ligand. The measured shift of approximately 5 cm^{-1} compares well with the 8-cm^{-1} shift predicted if the vibration is assumed to be a stretching mode between the iron and a rigid CN^- ligand. Figure 5b compares the resonance Raman spectra of CN^- metHb A with ^{12}C and ^{13}C in the ligand. The similar shift seen in the 452-cm^{-1} vibration serves to confirm the identification of this mode as the stretching vibration of the Fe–CN bond. In addition, in the 377-cm^{-1} line there is a change in width and slight shift (about 0.5 cm^{-1}) of the center frequency. Sensitivity of a Raman frequency to isotopic substitution of only one atom of a diatom pair has been shown by Yu et al. (N. T. Yu, B. Benko, E. Kerr, and K. Gersonde, unpublished results) to be characteristic of a bending mode. We attribute this difference to the presence of a Fe–C–N bending mode in this region mixed with a heme mode.

A substitution of ^{15}N for ^{14}N was also made in the NO_2^- ligand of NO_2^- metHb A (see paragraph at end of paper regarding supplementary material). No evidence was found for a resonantly enhanced iron–ligand mode in the low-frequency region, but a high-frequency mode at 1324 cm^{-1} was identified as an internal mode of the bound ligand. The frequency of this vibration falls within the range of frequencies of symmetric stretching modes of NO_2^- ligands in transition metal complexes, in which the ligand nitrogen is bound to the metal (Ferraro, 1971). For complexes in which the ligand is attached to the metal via an oxygen, no characteristic vibrational frequencies are found in the 1300–1400-cm^{-1} region (Ferraro, 1971). Our results then suggest that the ligand in NO_2^- metHb A is bound to the heme iron by its nitrogen.

^{13}C was substituted for ^{12}C in the SCN^- ligand in SCN^- metHb A (see paragraph at end of paper regarding supplementary material). A mode at 510 cm^{-1} shifts down-frequency in $S^{13}CN^-$ metHb from its position in $S^{12}CN^-$ metHb. This vibration is at a rather high frequency to be an iron–ligand stretch for such a massive ligand (Ferraro, 1971). It has been tentatively identified as an internal ligand bending mode on the basis of the appearance of such vibrations at similar frequencies in transition metal–isothiocyanate complexes (Bennett et al., 1967; Sabatini & Bertini, 1965). This assignment is consistent with the X-ray crystallographic observation that thiocyanate is coordinated to the iron in methemoglobin ex-

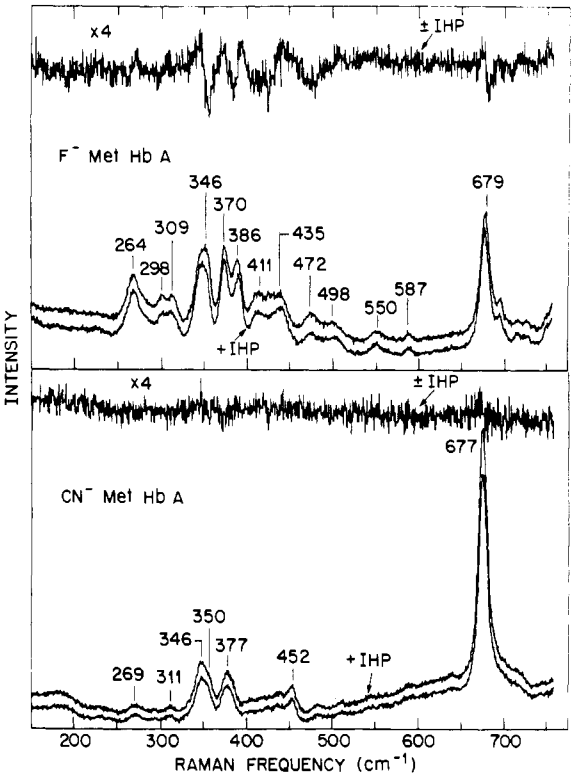

FIGURE 3: Resonance Raman spectra of the F^- and CN^- methemoglobin A derivatives in the low-frequency region. Conditions were the same as in Figure 1.

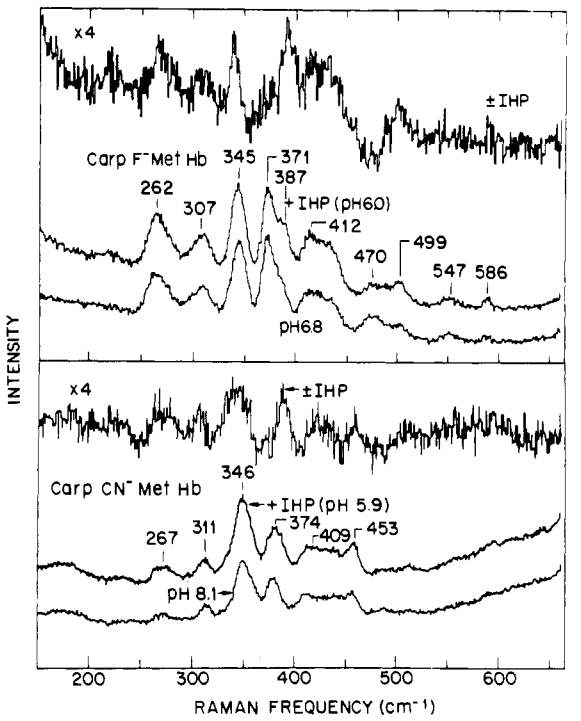

FIGURE 4: Resonance Raman spectra of the F^- and CN^- carp metHb derivatives in the low-frequency region. Conditions were the same as in Figure 1.

clusively by its nitrogen atom, thus forming the isothiocyanate complex (Korszun & Moffat, 1981).

Absorption and CD Spectra

UV Absorption Spectra. The UV difference spectra of concentration-matched samples of liganded methemoglobins of adult human and carp [(Hb + IHP) − (Hb stripped)] were measured at fixed pH (see paragraph at end of paper regarding

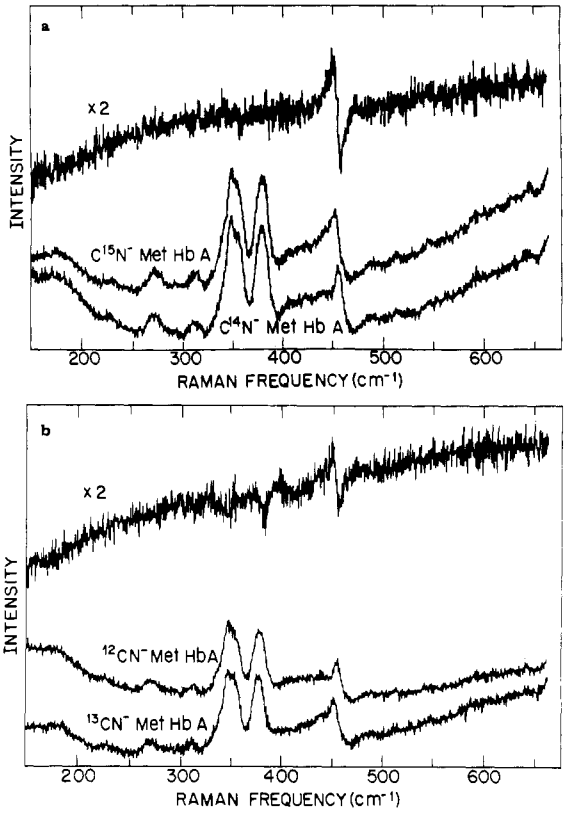

FIGURE 5: Isotope substitutions on the ligand in CN^- metHb A. The difference spectra at the top of both panels are (substituted) − (normal). (a) $^{12}C^{15}N^-$ metHb vs. $^{12}C^{14}N^-$ metHb. (b) $^{13}C^{14}N^-$ metHb vs. $^{12}C^{14}N^-$ metHb. Conditions were as in Figure 1.

supplementary material). The spectra of the liganded metHb A derivatives were similar to those published previously (Perutz et al., 1974a). All difference spectra have in common peaks at 278 and 287 nm. The difference spectra of all methemoglobins A display a feature of varying size in the 300–305-nm region, and the difference spectra of SCN^-, H_2O, and F^- metHb A also have a feature at 294 nm. The UV difference spectra of carp methemoglobins (Figure 6) differ from those of methemoglobins A in the complete absence of a 294-nm feature and a broader 287-nm peak in the carp proteins.

An interesting pH dependence is exhibited by the difference spectra of certain of the carp metHbs. The difference spectrum of SCN^- carp metHb measured at pH 6.0 (not shown) is roughly 5 times smaller than that measured at pH 6.7, in effective agreement with previously reported results (Perutz et al., 1978). In addition, the difference spectra of F^- and H_2O carp metHb at pH 6.0 are somewhat smaller than the corresponding spectra at pH 6.8 (Figure 6).

Visible Absorption Spectra. Absorption of light in the 350–700-nm spectral region by hemoglobin is entirely due to the heme. Figures 7 and 8 show the IHP-induced difference spectra in the visible (460–700-nm) region for the human and carp methemoglobins under the same conditions as were described for the UV difference spectra (see paragraph at end of paper regarding supplementary material). From the difference spectra, the effect of IHP on the visible absorption spectra of most of the methemoglobin derivatives studied is a red shift and/or increase in intensity of the absorption band in the 600–650-nm region, a decrease in intensity of bands in the 530–600-nm region, and red shifts and increases in intensity of a band in the 480–530-nm region.

The most striking comparison between the carp and human proteins is in the N_3^- derivatives, for which the visible difference spectra are several times larger in carp Hb than in Hb

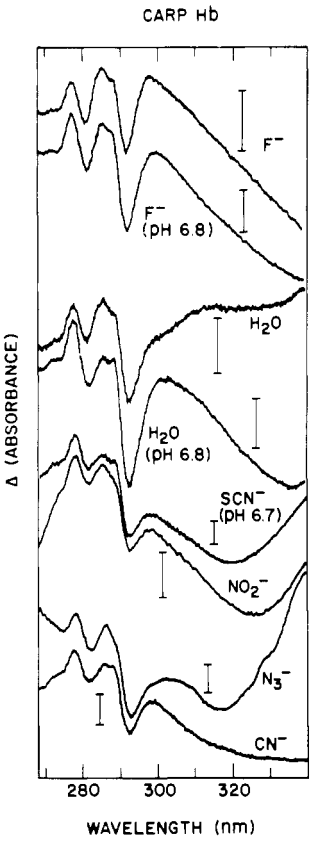

FIGURE 6: UV optical absorption difference spectra of the liganded carp methemoglobin derivatives. Differences are (metHb A derivative + 4–10-fold molar excess of IHP) – (stripped metHb A derivative). Conditions were heme concentration of 200 μM in 0.1 M Bis-Tris-buffered solutions, pH 5.9–6.1 (unless otherwise indicated). The vertical bar next to each spectrum represents a difference in extinction coefficient of 0.2 mM^{-1} cm^{-1}.

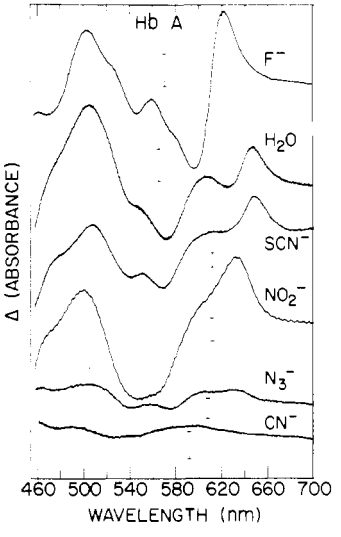

FIGURE 7: Optical absorption difference spectra of methemoglobin A derivatives in the visible wavelength region, (derivative + 4–10-fold molar excess of IHP) – (derivative stripped). Conditions were as in Figure 6, except that the pH was 6.3. The vertical bar with each spectrum represents a difference in extinction coefficient of 0.2 mM^{-1} cm^{-1}.

A. The difference spectra of the NO_2^- derivatives are both quite large, in the carp protein sufficiently so that an IHP-induced color change could be seen with the naked eye, as noted previously (Perutz et al., 1978). As in the UV spectra, the visible difference spectra of H_2O and F^- carp metHbs at pH 6.8 are larger than those at pH 6 and much closer in size

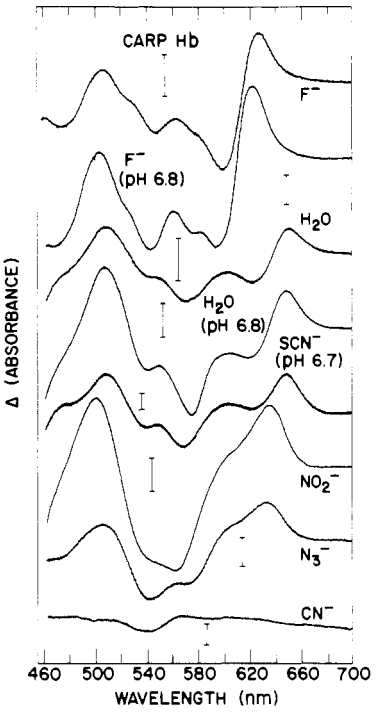

FIGURE 8: Optical absorption difference spectra of the carp methemoglobin derivatives in the visible wavelength region, (derivative + 4–10-fold molar excess IHP) – (derivative stripped). The vertical bar with each spectrum represents a difference in extinction coefficient of 0.2 mM^{-1} cm^{-1}. pH is 5.9–6.1 unless otherwise indicated.

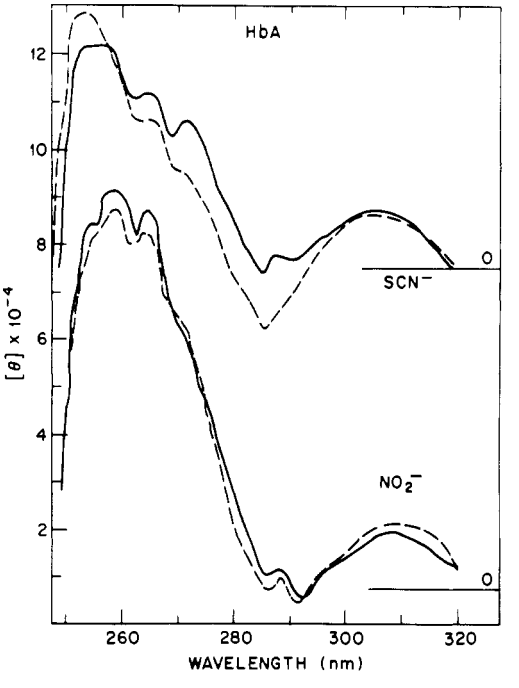

FIGURE 9: Circular dichroism spectra of methemoglobin A derivatives in the UV wavelength region. Solid lines are the spectra of the stripped derivatives; dashed lines are for 1 mM IHP added. pH is 6.0. These data were gathered by making three separate determinations for each methemoglobin, and the three data sets were numerically averaged at every 2.5 nm. The plots in this figure and in Figure 10 were generated by connecting the averaged points. The spectra of the derivatives not shown here (F^-, H_2O, N_3^-, and CN^-) have been reported by Perutz et al. (1974a).

to the difference spectra of the corresponding metHbs A.

CD Spectra. The circular dichroism (CD) spectra of various methemoglobin derivatives both with and without IHP in the 260–320-nm region are shown in Figures 9 and 10. The

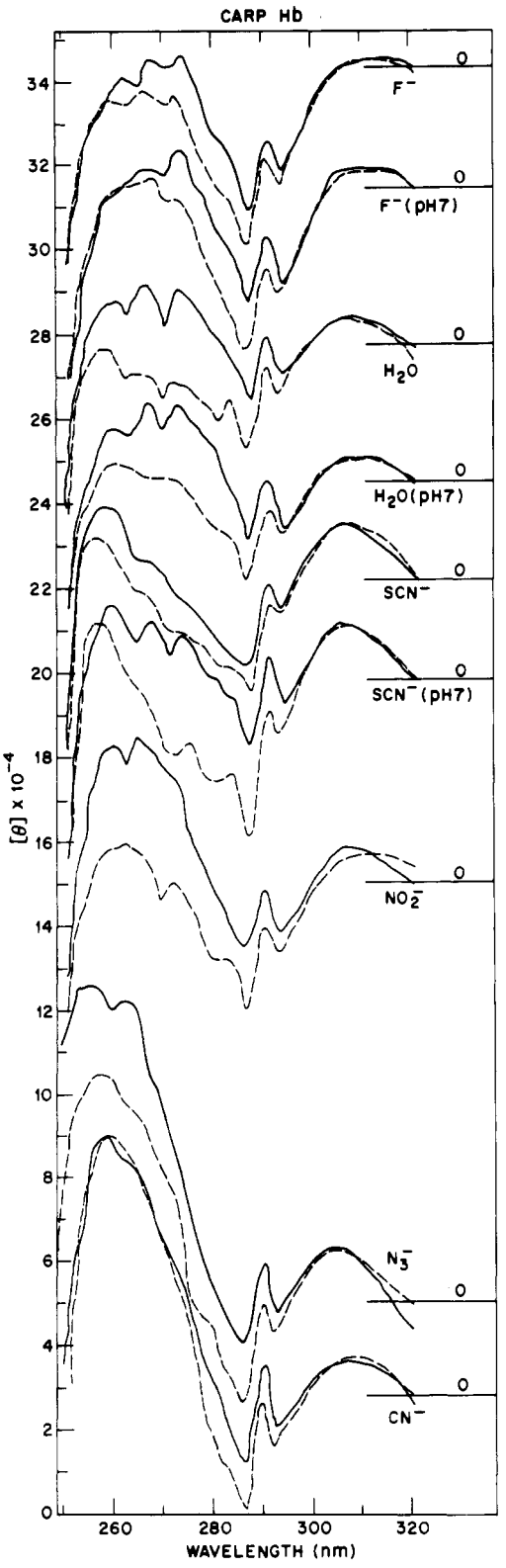

FIGURE 10: Same as Figure 9, for the carp methemoglobin derivatives. pH is 6.0 unless otherwise indicated.

spectra of F^-, H_2O, CN^-, and N_3^- metHb A are not shown here, as they have appeared previously in the literature (Perutz et al., 1974a). In SCN^-, H_2O, and F^- metHb A a single negative ellipticity peak appears at 287 nm in the +IHP spectra which does not appear in the corresponding −IHP spectra. The +IHP spectra of all the carp metHb derivatives display a substantial deepening of a "trough" at zero or small negative ellipticity which appears in the spectra of the proteins without IHP.

Discussion

IHP-Induced Changes in Quaternary Structure

There are several physicochemical probes that have been reported to be useful as indicators of quaternary structure in methemoglobins. These include probes of chemical reactivity of specific groups within the protein [e.g., sulfhydryl reactivity (Perutz et al., 1974a)] and spectroscopic changes in the globin [e.g., UV absorption, CD, and NMR (Perutz et al., 1974a; Fung & Ho, 1975)] and on the heme [Raman, visible, and near-UV absorption (Rousseau et al., 1980a; Perutz et al., 1974b)]. Most often only one such probe has been used in studies of methemoglobins, rather than utilizing several from which intercomparisons may be made. In the work reported here, IHP-induced changes were studied for stable liganded derivatives of human and carp methemoglobins by the techniques of Raman scattering, UV and visible absorption spectroscopy, and circular dichroism.

In assessing the structural significance of IHP-induced changes detected by these various techniques, it should be pointed out that the response of the liganded derivatives of carp methemoglobin to IHP binding is different from that of the derivatives of methemoglobin A. Specifically, all derivatives of carp methemoglobin are reported to be switched from the R to the T quaternary structure when IHP is bound (Perutz et al., 1978), independent of the spin state or other electronic properties conferred on the iron by the bound ligand, whereas only those derivatives of methemoglobin A in which the iron is predominantly high spin are apparently switched by IHP binding (Perutz et al., 1978).

Raman Spectra. It was suggested by Rousseau et al. (1980a) that the magnitude of the frequency shift of the polarized Raman line in the 1350–1400-cm^{-1} region is a signature of the quaternary structure change induced by IHP binding to the protein. A refinement of this picture is suggested by the additional data reported here. We have observed that the line width is significantly greater for those methemoglobins known to exist in a thermal mixture of low-spin and high-spin states of the heme iron than in those known to be primarily in one spin state or the other, based upon measured magnetic susceptibilities (Havemann & Haberditzl, 1958) (see paragraph at end of paper regarding supplementary material). This observation suggests that this vibrational mode displays different frequencies for hemes with irons of different spins. Thus, a thermal mixture of spin states will result in a broader line than will a pure spin state, and a change in the relative populations of the two spin states will lead to an apparent change in frequency and/or shape of the line. Furthermore, it appears that the high-spin component (lower frequency) of this line is more sensitive to IHP-induced protein structural changes than the low-spin component. From our observations it is evident that the 1370-cm^{-1} line is very sensitive to a variety of globin influences on the heme. In addition to the apparent sensitivity to spin state noted above, a sensitivity to tertiary structural changes upon binding IHP in the absence of spin-state changes or quaternary structure changes is also indicated by the differences detected in the CN^- and N_3^- metHb A spectra. Finally, this line is sensitive to quaternary structure changes in the absence of significant spin-state changes as evidenced by the large change it undergoes on the addition of IHP to F^- metHb A. Owing to the diversity of response of this line, its specificity as a quaternary structure marker for methemoglobins as proposed earlier (Rousseau et al., 1980a) is questionable.

The Raman spectra in the 100–600-cm^{-1} region contain several broad and closely spaced lines. Moreover, the structure

of the spectrum in this region depends on the particular ligand which is bound, and certain lines have contributions from the iron–ligand stretching modes. Examination of the quaternary structure dependence in the low-frequency region reveals that there are systematic differences in the frequencies and intensities of modes in this region. For F^-, H_2O, and SCN^- metHb A a characteristic difference spectrum is seen in which there are peaks near 340, 360, and 380 cm^{-1} and valleys near 350 and 370 cm^{-1}. The magnitudes of any differences in this region are very much smaller in NO_2^- metHb A and are nearly nonexistent in CN^- and N_3^- metHb A. As will be discussed below, IHP does not induce a quaternary structure transition in the NO_2^-, CN^-, or N_3^- derivatives of human hemoglobin. The changes in the F^-, H_2O, and SCN^- derivatives are thus attributed to the quaternary structure transition.

Similar changes are seen in the carp derivatives, namely, an increase in intensity of lines near 340 and 380 cm^{-1} upon changing the quaternary structure. However, in this case the changes are detected in all the derivatives. Indeed, the magnitudes of the changes in the CN^- derivative are comparable to those in the F^- and H_2O derivatives. We conclude that these are systematic changes in the low-frequency region that are associated with the quaternary structure transition.

UV Difference Spectra. In both human and carp hemoglobins the absorption difference spectra in the region between 270 and 300 nm have characteristic shapes associated with the binding of IHP to the protein. Within this region in HbA the intensity difference between 283 and 287 nm appears to be the most reliable focus for quantitative measurements. Among the various derivatives there is a clear bimodal distribution of magnitudes of $\Delta\epsilon_{283} - \Delta\epsilon_{287}$, with one set having values greater than about 0.3 mM^{-1} cm^{-1} and the other set having values less than about 0.1 mM^{-1} cm^{-1}. The bimodality of the magnitude of this feature supports its use as a structural signature; the magnitude of the difference spectrum in this region has previously been cited as a crude indicator of quaternary structural change (Perutz et al., 1974a).

For carp Hb the qualitative appearance of the difference spectrum is quite different from that of Hb A, but again within the species a characteristic shape is observed. Here the most consistent feature in the difference spectra is the dip between 287 and 293 nm. In this case, the differences in $\Delta\epsilon$ between these two wavelengths for all the derivatives are larger than about 0.3 mM^{-1} cm^{-1}. Although strictly speaking we cannot apply to carp Hb the quantitative criterion suggested by the results for Hb A, the similar sizes of the UV difference spectra of all the carp derivatives suggest that we are seeing a signature of a quaternary structure transition in all cases.

CD Spectra. For human hemoglobin the ultraviolet CD spectra have been shown to be reliable indicators of quaternary structure (Simon & Cantor, 1969; Perutz et al., 1974a). By balancing to zero ellipticity at 320 nm, for the R structure the ellipticity remains positive in the 280–300-nm region and consists of a doublet with peaks at 293 and 286 nm. However, when the protein changes to the T quaternary structure, the doublet becomes a single peak at about 283 nm and has a significant excursion to negative ellipticity. Although these contributions are believed to result from changes in positions of aromatic residues of the globin, intensity differences in the 250–260-nm region appear to have contributions from the heme as well. This latter region responds strongly to spin state, having a larger ellipticity for low-spin hemoglobins and a much reduced contribution for high-spin hemoglobins.

The CD differences in carp Hb induced by the addition of IHP (Figure 10) are more difficult to assess. Changes in quaternary structure appear to be associated with negative ellipticity in the 280–290-nm region, but these changes are complicated by the broad changes to negative ellipticity in the 250–260-nm region presumably resulting from changes in the spin equilibrium. Structural features within this region further complicate the IHP-induced CD differences.

From the above analysis the effect of IHP on the quaternary structures of the various methemoglobin derivatives may be assessed. Previous workers had used changes in the optical absorption spectrum to assess the quaternary structure change and concluded that in human methemoglobin the F^-, H_2O, OCN^-, SCN^-, $SeCN^-$, NO_2^-, and imidazole derivatives could be switched to the T structure by IHP (Perutz et al., 1978). We have not examined the OCN^- and $SeCN^-$ derivatives. The imidazole derivative was reexamined previously, and on the basis of the UV difference spectrum, it was concluded that in the human protein this derivative could not be switched into the T structure (Rousseau et al., 1980b).

For NO_2^- metHb A the UV difference spectrum is quite different from those of the F^-, H_2O, and SCN^- derivatives. By all criteria these latter three derivatives change quaternary structure on the addition of IHP. The question of the switchability of the NO_2^- derivative is resolved by the CD spectra (Figure 9). The negative ellipticity for the SCN^- derivative in this region is clear and confirms the transition to the T structure induced by IHP. The CD spectra of the NO_2^- derivative display no such conversion to negative ellipticity, and we therefore conclude that IHP does not induce a change to the T quaternary structure in this derivative. The changes in the CD and the UV absorption spectra of the carp metHb derivatives are large and fully consistent with the view that all of these derivatives convert to the T structure in the presence of IHP.

Neya & Morishima (1981) presented NMR evidence suggesting structural heterogeneity in low-spin liganded derivatives (imidazole, N_3^-, and CN^-) of metHb A to which IHP is bound and proposed that this heterogeneity represented an equilibrium distribution of R and T conformers in solution at room temperature. In a subsequent paper, Neya et al. (1983) reported temperature-dependent studies that indicated that perhaps 25% of IHP-bound N_3^- metHb A is in the T state at room temperature. These results would suggest that IHP is able to stabilize the T state in some low-spin methemoglobin derivatives sufficiently to introduce a small but finite population of this state at the temperature at which we have made our measurements. In such cases a more quantitative study may be required in order to determine the precise degree of stabilization of the T state by IHP binding and whether or not there is in fact a finite population of T state in low-spin liganded derivatives at room temperature.

In general we have observed that the IHP-induced changes in the resonance Raman and optical absorption spectra of the F^-, H_2O, and SCN^- derivatives of carp methemoglobin are significantly smaller at pH 6.0 than at pH 6.8 or higher. We have also observed that the Raman and absorption spectra of these derivatives are sensitive to pH changes alone in the absence of IHP; in the carp F^- and SCN^- derivatives the spectral differences between pH 6.0 and pH 6.8 are in some cases comparable in size to the IHP-induced differences at the higher pH. These results suggest that an increased binding of protons alone is sufficient to bring about a large shift in the structural equilibrium toward the T state in at least some of the carp methemoglobin derivatives.

IHP-Induced Changes in Spin Equilibrium

The Raman lines in the 1450–1650-cm^{-1} region of the

Table I: IHP-Induced Changes in Spin Equilibria of Methemoglobins

		from magnetic susceptibilities		from Raman measurements[c]			
ligand	±IHP	magnetic moment[a]	% HS[b]	% HS	ΔHS	ΔG (kcal/mol)	ΔΔG (kcal/mol)
				MetHb A			
F^-	−	5.78	95	100	0 (±1)		
	+			100			
H_2O	−	5.60	89	83 (±3)	5 (±1)	0.92	0.24
	+			88 (±4)		1.16	
SCN^-	−	5.12	73	71 (±1)	9 (±1)	0.52	0.29
	+			80 (±5)		0.81	
NO_2^-	−	4.13	44	40 (±5)	4 (±1)	−0.24	0.10
	+			44 (±2)		−0.14	
N_3^-	−	2.87	16	6 (±6)	1 (±1)	−1.60	0.09
	+			7 (±5)		−1.51	
CN^-	−	2.37	7	0	0 (±1)		
	+			0			
				Carp MetHb			
F^-	−	5.82	97	98 (±3)	1 (±1)	2.26	0.42
	+	5.83	97	99 (±2)		2.68	
H_2O	−	5.72	93	92 (±6)	3 (±1)	1.42	0.29
	+	5.87	98	95 (±5)		1.71	
SCN^-	−			76 (±2)	12 (±5)	0.67	0.49
	+			88 (±3)		1.16	
NO_2^-	−	4.67	59	60 (±4)	29 (±3)	0.24	0.98
	+	5.52	86	89 (±1)		1.22	
N_3^-	−	2.77	15	7 (±5)	18 (±3)	−1.51	0.87
	+	4.24	47	25 (±8)		−0.64	
CN^-	−	2.62	12	0	9 (±2)		
	+	2.62	12	9 (±2)		−1.35	

[a] In Bohr magnetons (μ_B). Values used for the metHb A derivatives are from susceptibilities measured by Havemann & Haberditzl (1958). Values for the carp metHb derivatives are from Noble et al. (1984). [b] Calculated by using eq 1. HS is the population of the high-spin state. [c] Calculated as described in the text.

spectrum display differences in intensity from one liganded derivative to another and in some cases changes in relative intensity upon addition of IHP. Scholler & Hoffman (1979) used the changes in intensities of lines in this region to detect and quantify the IHP-induced changes in the high/low-spin equilibrium of N_3^- carp metHb. The relative intensities of the pair of lines at about 1480 and 1504 cm^{-1} scale roughly with the high- and low-spin contributions, respectively, as do the intensities of the pair at about 1565 and 1585 cm^{-1}. Most of the high-frequency Raman spectra presented here display changes in the relative intensities of the lines, suggesting at least small IHP-induced changes in spin equilibrium in nearly all the liganded methemoglobins. The use of the intensities of these lines to determine relative high-spin/low-spin concentrations is complicated by the presence of overlapping lines, clearly indicated by "extra" peaks in some spectra (e.g., the spectrum of SCN^- carp metHb shows an extra peak in the 1500–1520-cm^{-1} region) and verified by depolarization ratio studies in which multiple components could be clearly discerned. Thus, none of the "marker" lines for one spin state completely vanish upon total conversion to the other spin state. However, keeping the above restrictions in mind, rough estimates for the relative spin populations may be made from the Raman intensities in this region.

To determine the fraction of high (or low) spin in a given sample, we have used the lines both in the 1480–1510-cm^{-1} region and in the 1565–1585-cm^{-1} region of the Raman spectra. For each pair of lines we have necessarily assumed that the intrinsic intensity of the high-spin peak is the same as that of the low-spin peak. For each set of lines and for each species we have used as a reference line (fully high spin or low spin) that sample which by the criteria of these lines had the highest or lowest spin. The assessments of the spin distribution from each of the two sets of marker lines did not precisely agree. Thus, for example, in carp metHb for the 1481/1517-cm^{-1} set we have taken the F^- derivative + IHP as being fully high spin. For analysis of the 1564/1581-cm^{-1} set, the H_2O carp metHb + IHP had a larger high-spin population than did the F^- derivative so it was taken as the high-spin reference. In making the determination of the spin equilibrium it was assumed that the background at each frequency could be subtracted out and that the background intensity was independent of the spin state.

In Table I the spin equilibria of metHbs A are listed for the various ligands that were examined. These data were obtained by averaging the measurements from the two sets of lines. The cited uncertainties represent the differences between these two sets. The ligands range from fully high spin (F^-) to fully low spin (CN^-). To assess the relationship between the spin equilibria obtained from the Raman data and those obtained from direct susceptibility measurements, we have calculated the fraction of high spin (α) from the magnetic moments (μ) calculated from the susceptibility measurements reported by Havemann & Haberditzl (1958) for metHb A derivatives. We have used a low-spin magnetic moment of 1.73 μ_B and a high-spin value of 5.9 μ_B. The fractional population of the high-spin state may then be written as

$$\alpha = (\mu^2 - 3)/32 \quad (1)$$

The form of this equation depends upon the choices made for the magnetic moment values of the low-spin and high-spin states, which may be greater than the spin-only values because of orbital angular momentum contributions, particularly in the low-spin state. Increasing the low-spin magnetic moment from 1.73 to 2.0 (Messana et al., 1978) has only a small effect on the calculated fractional high-spin populations, so we have used the spin-only value of 1.73 for all of the calculations. The agreement between the fraction of high spin obtained from the Raman data and that obtained in this way from the susceptibility measurements is excellent (Table I). Thus, for the

human hemoglobins the Raman intensities appear to be a reliable measure of the spin distribution.

On adding IHP to the metHbs A the spin equilibria for all the samples were shifted toward a larger high-spin population. The increases in the fractional high-spin populations (ΔHS) due to the presence of IHP are listed in a separate column in Table I. The errors listed in this column represent the differences between the IHP-induced changes in spin equilibrium determined from the two sets of Raman lines. These errors are generally smaller than the error in the determination of the spin equilibrium for a given sample. In other words, the change in spin equilibrium on addition of IHP as determined by the two sets of lines gave more consistent results than did the absolute determination of the spin equilibrium. The SCN^- derivative displayed the largest IHP-induced difference in spin equilibrium with smaller differences detected in the H_2O and NO_2^- derivatives and negligible differences for the other ligands.

This spin equilibrium analysis was also carried out for the carp metHb derivatives, and the results are summarized in Table I. Again a distribution of spin equilibria is found. IHP always induces an increase in the fractional high-spin population, with very large changes in spin equilibrium occurring in the NO_2^- and N_3^- derivatives.

From the spin equilibria the relative free energies of the high- and low-spin states may be calculated by using

$$[LS]/[HS] = e^{-\Delta G/k_BT} \quad (2)$$

where [HS] and [LS] are the concentrations of the high-spin and low-spin species, respectively, and ΔG is the free energy difference between the low-spin and the high-spin states, positive for a more stable high-spin state. The values of ΔG calculated from our data are also listed in Table I.

The quantity $\Delta\Delta G$ is the change in ΔG induced by IHP binding. For most of the methemoglobins the spectral and Raman changes at the heme upon the addition of IHP are most closely correlated with the change in equilibrium expressed by $\Delta\Delta G$ and less strongly linked to the effect of the force of the protein on the heme geometry within a fixed spin state (i.e., the addition of IHP changes the high/low-spin equilibrium, but the frequencies of the Raman lines within a given spin state change very little). Whether these forces or their concomitant $\Delta\Delta G$ values are entropic or enthalpic cannot be determined from spectroscopy at one temperature.

The free energy difference ΔG between high-spin and low-spin states can be conceptually partitioned into three parts. First, there is an entropic contribution from the difference in the spin-state degeneracies. Second, there is a term, probably chiefly enthalpic, that would occur even if the protein did not produce constraints on the heme and proximal histidine. Third, there is a term representing the work done by the heme and direct ligand geometry changes against the protein forces of constraint. This third term will be temperature dependent (i.e. will have an entropic contribution) if the forces of the protein on the heme–ligand complex are temperature dependent. In flexible polymers (Flory, 1953), such forces typically have large temperature dependences—the force of a stretched rubber band is nearly proportional to T and is chiefly an entropic effect–and thus, it would not be surprising for there to be such terms in proteins. The large values of ΔS observed in high-spin–low-spin equilibria in heme proteins (Iizuka & Kotani, 1969) are probably explicable in such terms. In considering the effect of IHP on the spin equilibria, it is important to note that it will operate through the third contribution, whether or not it changes the quaternary structure.

Figure 11 plots the data in such a way that the implications

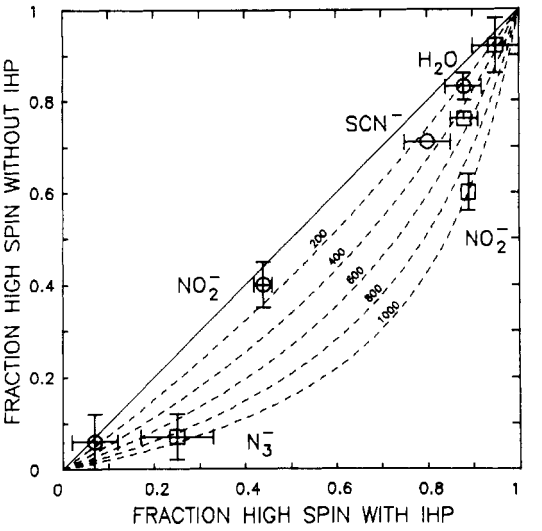

FIGURE 11: Effect of IHP on the spin equilibria of methemoglobin derivatives, plotted as the fraction of high spin in the derivative with IHP vs. the fraction of high spin in the stripped derivative. The high-spin populations plotted are determined from the Raman measurements as described in the text and listed in Table I. Data plotted as a circle (○) are for methemoglobin A derivatives, and those plotted as a square (□) are for carp methemoglobin derivatives. Error bars that would lie entirely inside the plotted circle or square have been deleted. The dashed lines (- - -) are contours defined by $[y/(1-y)]/[x/(1-x)] = e^{-\Delta\Delta G/(k_BT)}$ for various constant values of $\Delta\Delta G$ (see text), where y is the fractional high-spin population without IHP and x is the fractional population with IHP. Each contour is labeled with the value of $\Delta\Delta G$ in calories per mole.

of the measurements on $\Delta\Delta G$ can be readily seen. For Hb A, the addition of IHP has no measurable $\Delta\Delta G$ (within experimental accuracy) when there is no quaternary structure change (N_3^-) and is consistent with a $\Delta\Delta G$ of about 300 ± 100 cal/mol when the quaternary structure changes (H_2O and SCN^-). F^- and CN^-, for which values of ΔG and $\Delta\Delta G$ cannot be computed, are consistent with this description but do not add to it. For carp hemoglobin, in which all liganded derivatives are believed to undergo a quaternary structure change, the $\Delta\Delta G$ is larger and consistent with a value of 600 ± 100 cal/mol for all the derivatives shown.[2] Within our experimental accuracy we are unable to establish a ligand dependence of $\Delta\Delta G$ in Hb A or carp hemoglobin. This conclusion is consistent with that of Noble et al. (1984), who have suggested that $\Delta\Delta G$ is ligand independent.

Comparing the spin equilibrium results for metHb A and carp metHb derivatives reveals an important systematic difference between these proteins. For those ligands that confer a thermal mixture of high- and low-spin states to the heme iron at room temperature, the carp metHb derivatives have a larger fractional high-spin population than the corresponding metHb A derivatives; i.e., the high-spin configuration has a lower energy relative to the low-spin configuration in the carp

[2] There are sources of additional uncertainty, not included in the error bars in Figure 11, in the calculated high-spin fractions for certain of the liganded derivatives. For example, the NO_2^- derivatives of methemoglobins are unstable because of the strong oxidizing properties of the anion, so our data acquisition times are necessarily short for these derivatives. This reduces the quality of the measured spectra, introducing large uncertainties in our determinations of the relative intensities of spin-state marker lines for this ligand. Furthermore, the pH dependence of the structural and spin-state equilibria of some carp methemoglobin derivatives suggests that estimates of the IHP effect on spin equilibria made from measurements at low pH (e.g., H_2O carp metHb) may be too low because of a partial spin-state transition in these derivatives at low pH even in the absence of IHP.

metHbs than in the metHbs A, under all conditions that we have examined.

Changes in Visible Absorption Spectra

The IHP-induced difference spectra of metHb A (Figure 7) and carp metHb (Figure 8) derivatives raise some interesting points. Within one type of protein, the variation in the difference spectrum from one ligand to another is very large. However, in comparing the difference spectra for the same ligand between human and carp Hb, it is the similarities that are most striking, in spite of large differences in the individual absorption spectra (see paragraph at end of paper regarding supplementary material). This even holds in the NO_2^- derivatives, in which the spin equilibria, and changes therein upon IHP binding, are both quite different.

On the basis of these comparisons we conclude that (1) the bound ligand strongly influences the heme response to protein binding of IHP, (2) large changes in heme absorption spectra may occur in the absence of changes in quaternary structure or spin equilibrium, and (3) the addition of IHP exerts very similar forces on the heme for many of the liganded forms of the human and carp methemoglobins.

Our observations that the effects of IHP on the absorption spectra are very ligand dependent and much less protein dependent are in marked contrast to the changes in the low-frequency Raman spectra. The latter differences give a clear indication of changing quaternary structure. The absorption differences are much less reliable markers of protein quaternary structural change. The absolute absorption spectra of the various liganded methemoglobins are very different and do not reflect spin equilibria in a simple fashion. Thus, the electronic properties of the ground and/or the excited states of the porphyrin macrocycle are strongly determined by the ligand and not simply by the spin state that is imposes on the iron. The responses of the electronic properties to the structural changes induced by binding IHP are correspondingly different. From optical data it cannot be determined whether in a specific protein IHP exerts the same type of perturbation on the heme regardless of the bound ligand. However, the Raman data suggest that it does.

Mechanism of IHP Influence at the Heme

Our observations demonstrate that the addition of IHP lowers the energy of the high-spin state relative to the low-spin state independent of the protein or the bound ligand. These changes in spin equilibrium arise from the coupling of IHP binding by the protein to changes in the energies and/or statistical factors of heme electronic states involving the iron d orbitals by means of IHP-induced structural changes in the protein. Possible mechanisms for this coupling include (1) an out-of-plane displacement of the iron atom induced by tension between the histidine and the porphyrin, (2) stretching of the iron–histidine bond by protein structural changes without significant motion of the iron atom, (3) changes in the structure and electronic properties of the porphyrin induced by tertiary structural changes in the heme pocket, and (4) changes in the orientation of the proximal histidine with respect to the porphyrin plane.

These possibilities may be assessed with the aid of the data reported here and elsewhere. First of all, our results and those of other studies clearly show that the bond between the iron and the exogenous ligand is not affected by the addition of IHP. We have detected no change in the Fe–CN stretching mode, which was clearly identified in our isotope substitution studies on CN^- metHb A, upon the addition of IHP to CN^- carp metHb. Furthermore, no IHP-induced frequency changes were seen in other iron–ligand modes of methemoglobins reported by other workers (Asher et al., 1977; Desbois et al., 1979; Asher & Schuster, 1979; Tsubaki et al., 1981). Likewise, no changes in iron–ligand modes have been detected in ferrous hemoglobin when the quaternary structure is changed by IHP (Nagai et al., 1980b; Tsubaki et al., 1982; Rousseau et al., 1984). Inferences concerning both the iron position with respect to the heme plane and the iron–histidine bond length may be drawn from these data as follows.

Calculations have shown that the position of the iron is primarily controlled by the nonbonded interactions between the histidine and the porphyrin and between the exogenous ligand and the porphyrin (Warshel, 1977; Olafson & Goddard, 1977). Therefore, any change in out-of-plane position of the iron would be expected to change the nonbonded interactions between the exogenous ligand and the porphyrin and thereby influence the iron–ligand stretching mode frequency. That we detect no such frequency change suggests that IHP binding to methemoglobins and the resulting spin equilibrium and/or quaternary structure changes do not result in a significant out-of-plane motion of the iron, although it is difficult to estimate quantitatively how large such a motion could be and still cause a change in the frequency of an iron–ligand mode below our limits of detection. Furthermore, Korszun & Moffat (1981) concluded from comparisons of spin states of various methemoglobins that iron out-of-plane motion is not necessarily correlated with spin state. Thus, we exclude the above possibility 1 that the iron out-of-plane position determines the spin equilibrium.

If the iron–histidine bond were stretched significantly by the protein upon adding IHP, a significant trans effect, i.e., modification of the Fe–ligand bond, would be expected (Rousseau et al., 1984), as well as some iron out-of-plane motion. Therefore, from the apparent absence of these effects in cyanomethemoglobins we infer that significant stretching of the iron–histidine bond is not occurring, ruling out possibility 2.

The changes in the low-frequency modes which we report here suggest that IHP-induced changes in the heme environment influence groups on the heme periphery, since the peripheral groups tend to contribute to these normal modes. Furthermore, in all hemoglobins studied, the addition of IHP induces changes in the porphyrin electron density marker line (1350–1380 cm^{-1}). This is taken as evidence for changes in the porphyrin π orbitals. Since these are mixed with the iron d orbitals, changes in the porphyrin electronic structure can influence iron d orbital energies and thus may also influence the spin equilibrium. Indeed, Scheidt et al. (1979) have proposed an association between the spin equilibrium and heme contraction. Thus, from our data as well as other data possibility 3 cannot be excluded.

Finally, the fourth possibility, that of orientational changes of the histidine with respect to the porphyrin, is also consistent with our data. Such changes occur in the deoxyhemoglobins and might well also occur in the methemoglobins. Overall, we conclude that tertiary structural changes occur upon binding IHP which affect the porphyrin and histidine leading to the change in spin equilibrium. These may be structural changes in the porphyrin or orientational changes in the histidine which affect energies but not the position of the iron atom. The changes in orbital energies bring about the shift in the spin equilibrium. Although further elucidation of the mechanism is not possible from our data, the similar type of response for both human and carp methemoglobins indicates that the mechanism of IHP control of the spin equilibrium may

be the same for each protein but the magnitude of the effect is different.

Supplementary Material Available

Resonance Raman spectra of the metHb A and carp metHb derivatives in the 1350–1400-cm^{-1} frequency region and in the frequency region below 600 cm^{-1}, results of isotopic substitution experiments in NO_2^- and SCN^- metHb A, UV absorption difference spectra and absolute visible absorption spectra of the metHb A and carp metHb derivatives, and tabulated properties of the 1370-cm^{-1} Raman line for the various derivatives (11 pages). Ordering information is given on any current masthead page.

Registry No. IHP, 83-86-3; ^{15}N, 14390-96-6; ^{13}C, 14762-74-4; fluorometHb A, 54577-85-4; aquometHb A, 61008-19-3; thiocyanatoHb A, 72175-40-7; nitritometHb A, 74665-89-7; azidometHb A, 9072-23-5; cyanometHb A, 39340-60-8; heme, 14875-96-8.

References

Abe, M., Kitagawa, T., & Kyogoku, Y. (1978) *J. Chem. Phys. 69*, 4526–4534.

Allen, D. W., Schroder, W. A., & Balog, J. (1958) *J. Am. Chem. Soc. 80*, 1628–1634.

Asher, S. A., & Schuster, T. M. (1979) *Biochemistry 18*, 5377–5387.

Asher, S. A., Vickery, L. E., Schuster, T. M., & Sauer, K. (1977) *Biochemistry 16*, 5849–5856.

Baldwin, J. M. (1975) *Prog. Biophys. Mol. Biol. 29*, 225–320.

Baldwin, J. M., & Chothia, C. (1979) *J. Mol. Biol. 129*, 175–220.

Bennett, M., Clark, R., & Goodwin, A. (1967) *Inorg. Chem. 6*, 1625–1631.

Brunner, H. (1974) *Naturwissenschaften 61*, 129.

Cho, K. C., Remba, R. D., & Fitchen, D. B. (1981) *Biochim. Biophys. Acta 668*, 186–192.

Choi, S., & Spiro, T. G. (1983) *J. Am. Chem. Soc. 105*, 3683–3692.

Choi, S., Spiro, T. G., Langry, K. C., & Smith, K. M. (1982a) *J. Am. Chem. Soc. 104*, 4338–4344.

Choi, S., Spiro, T. G., Langry, K. C., Smith, K. M., Budd, D. L., & LaMar, G. N. (1982b) *J. Am. Chem. Soc. 104*, 4345–4351.

Desbois, A., Lutz, M., & Banerjee, R. (1979) *Biochemistry 18*, 1510–1518.

Ferraro, J. (1971) *Low Frequency Vibrations of Inorganic and Coordination Compounds*, Plenum Press, New York.

Flory, P. J. (1953) *Principles of Polymer Chemistry*, p 439, Cornell University Press, Ithaca, New York.

Fung, L. W.-M., & Ho, C. (1975) *Biochemistry 14*, 2526–2535.

Gelin, B. R., & Karplus, M. (1977) *Proc. Natl. Acad. Sci. U.S.A. 74*, 801–805.

Gelin B. R., Lee, A. W.-M., & Karplus, M. (1983) *J. Mol. Biol. 171*, 489–559.

Havemann, R., & Haberditzl, W. (1958) *Z. Phys. Chem. (Leipzig) 209*, 135–161.

Hopfield, J. J. (1973) *J. Mol. Biol. 77*, 207–222.

Iizuka, T., & Kotani, M. (1969) *Biochim. Biophys. Acta 194*, 351–363.

Korszun, Z. R., & Moffat, K. (1981) *J. Mol. Biol. 145*, 815–824.

Messana, C., Cerdonio, C., Shenkin, P., Noble, R. W., Fermi, G., Perutz, R. N., & Perutz, M. F. (1978) *Biochemistry 17*, 3652–3662.

Nagai, K., Enoki, Y., & Kitagawa, T. (1980a) *Biochim. Biophys. Acta 624*, 304–315.

Nagai, K., Kitagawa, T., & Morimoto, H. (1980b) *J. Mol. Biol. 136*, 271–289.

Neya, S., & Morishima, I. (1981) *J. Biol. Chem. 256*, 793–798.

Neya, S., Hada, S., & Funasaki, N. (1983) *Biochemistry 22*, 3686–3691.

Noble, R. W., Vitale, S., DeYoung, A., Morante, S., & Cerdonio, M. (1984) in *Hemoglobin Structure and Function* (Schnek, A. G., Ed.) pp 223–233, University Press, Brussels.

Olafson, B. D., & Goddard, W. A. (1977) *Proc. Natl. Acad. Sci. U.S.A. 74*, 1315–1319.

Perutz, M. F. (1970) *Nature (London) 228*, 726–734.

Perutz, M. F., Fersht, A. R., Simon, S. R., & Roberts, G. C. K. (1974a) *Biochemistry 13*, 2174–2186.

Perutz, M. F., Heidner, E. J., Ladner, J. E., Beetlestone, J. G., Ho, C., & Slade, E. F. (1974b) *Biochemistry 13*, 2187–2200.

Perutz, M. F., Sanders, J. K. M., Chenery, D. H., Noble, R. W., Pennelly, R. R., Fung, L. W.-M., Ho, C., Giannini, I., Porschke, D., & Winkler, H. (1978) *Biochemistry 17*, 3640–3652.

Pettigrew, D. W., Romeo, P. H., Tsapis, A., Thillet, J., Smith, M. L., Turner, B. W., & Ackers, G. K. (1982) *Proc. Natl. Acad. Sci. U.S.A. 79*, 1849–1853.

Rousseau, D. L. (1981) *J. Raman Spectrosc. 10*, 94–99.

Rousseau, D. L., & Ondrias, M. R. (1983) *Annu. Rev. Biophys. Bioeng. 12*, 357–380.

Rousseau, D. L., Shelnutt, J. A., Henry, E. R., & Simon, S. R. (1980a) *Nature (London) 285*, 49–51.

Rousseau, D. L., Shelnutt, J. A., & Simon, S. R. (1980b) *FEBS Lett. 111*, 235–239.

Rousseau, D. L., Ondrias, M. R., LaMar, G. N., Kong, S. B., & Smith, K. M. (1983) *Biochemistry 22*, 1740–1746.

Rousseau, D. L., Tan, S. L., Ondrias, M. R., Ogawa, S., & Noble, R. W. (1984) *Biochemistry 23*, 2857–2865.

Sabatini, A., & Bertini, I. (1965) *Inorg. Chem. 4*, 959–961.

Scheidt, W. R., Cohen, I. A., & Kastner, M. E. (1979) *Biochemistry 18*, 3546–3552.

Scholler, D. M., & Hoffman, B. M. (1979) *J. Am. Chem. Soc. 101*, 1655–1662.

Shelnutt, J. A., Rousseau, D. L., Friedman, J. M., & Simon, S. R. (1979) *Proc. Natl. Acad. Sci. U.S.A. 76*, 4409–4413.

Shelnutt, J. A., Rousseau, D. L., Dethmers, J. K., & Margoliash, E. (1981) *Biochemistry 20*, 6485–6497.

Simon, S. R., & Cantor, C. (1969) *Proc. Natl. Acad. Sci. U.S.A. 63*, 205–212.

Spiro, T., & Strekas, T. (1974) *J. Am. Chem. Soc. 96*, 338–345.

Spiro, T., & Burke, J. (1976) *J. Am. Chem. Soc. 98*, 5482–5489.

Tan, A. L., DeYoung, A., & Noble, R. W. (1972) *J. Biol. Chem. 247*, 2493–2498.

Tsubaki, M., Srivastava, R. B., & Yu, N.-T. (1981) *Biochemistry 20*, 946–952.

Tsubaki, M., Srivastava, R. B., & Yu, N.-T. (1982) *Biochemistry 21*, 1132–1140.

Warshel, A. (1977) *Proc. Natl. Acad. Sci. U.S.A. 74*, 1789–1793.